Ion implantation for quantitative ion microscopy of biological soft tissue. Anal Chem

ARTICLE *in* ANALYTICAL CHEMISTRY · NOVEMBER 1983

Impact Factor: 5.64 · DOI: 10.1021/ac00262a029 · Source: PubMed

3 AUTHORS, INCLUDING:

Subhash Chandra
Cornell University
78 PUBLICATIONS **1,688** CITATIONS

Ion Implantation for Quantitative Ion Microscopy of Biological Soft Tissue

William C. Harris, Jr., Subhash Chandra, and George H. Morrison*

Department of Chemistry, Cornell University, Ithaca, New York 14850

Quantitative ion implantation is used to produce a homogeneously distributed internal standard element in otherwise heterogeneous biological tissue samples. This allows quantification of ion microprobe data with an accuracy of 24%. Ion micrographs are acquired by use of an on-line digital acquisition system and subsequently processed to characterize the implanted internal standard element at each discrete location of the digitized image. This allows the pixel-by-pixel application of bulk quantification procedures based on the internal standard resulting in quantitative concentration maps of elemental distributions in biological soft tissues.

The increased sophistication of microanalytical techniques has facilitated not only studies of elemental concentrations in biological tissues but also the distribution of these elements within the tissue. Consequently, cytological localization of elements has become a major area of research. Histochemical information obtained by correlating morphological features with elemental distributions provides an increased understanding of the mechanisms of various biological processes and has important application in physiology, toxicology, and pathology.

Recently, the ion microscope, based on secondary ion mass spectrometry (SIMS), has become an increasingly attractive technique for these studies (*1*, *2*). The unique ion optics within the ion microscope produces a direct image of elemental distributions from an area up to 400 μm in diameter with lateral resolution approaching 0.5 μm. The instrument can also be operated in the microprobe mode of analysis in which the imaging capabilities are discarded and the entire field of view is summed into one analysis point. In this mode the instrument monitors changes in concentration or composition as a function of depth, with a depth resolution of 0.005–0.01 μm. Mass spectra of the sample can also be acquired in this mode from areas as small as 1 μm^2.

Although other microanalytical techniques such as electron microprobe are used in biological studies, they suffer from two main deficiencies: first, an inability to analyze for elements of low atomic numbers, and second, in many cases they provide inadequate sensitivity for the low concentration of elements found in biological systems. The ion microscope overcomes both these problems by offering coverage of the entire periodic table with sensitivities generally in the parts-per-million range. In addition, it provides geometric-fit ion images with sample histology. A variety of biological tissues have now been analyzed with ion microscopy (*3–7*), however, quantification of elemental distributions has remained an elusive goal.

Recent efforts to quantitate biological applications of SIMS have centered on the use of external calibration standards composed of a gelatin or plastic matrix doped with various concentrations of the elements of interest (*8*, *9*). These standards are used to generate a relative sensitivity factor or calibration line based on the ratio of signal intensity of the element of interest to a reference element which is also present in the standard. While analysis of these standards commonly yields linear calibration lines with good precision, their application to real biological samples has been largely unsuccessful due to the lack of reliable reference elements in the biological samples. The natural heterogeneity of biological tissues mitigates against finding an element which is either homogeneous or has a well-characterized heterogeneous distribution. This problem is particularly severe in the imaging mode where the reference element must be present in known concentration at each discrete point of the ion micrograph.

This study investigates the use of quantitative ion implantation to provide a reference element for ion imaging of biological soft tissue samples. Quantification of SIMS data by use of ion implantation of semiconductors has been described in detail elsewhere (*10–12*) and is capable of overcoming the lack of a well-characterized natural reference element in biological samples by introducing one by ion implantation. Quantitative interpretation of ion micrographs is facilitated by the use of the microscopic image digital acquisition system (MIDAS) for direct digitization of ion images (*13*). This system allows a series of digitized images of the implanted element to be collected. The image series spans the depth of the implant zone and permits the characterization of the implant at each picture element, or pixel, of the ion image. A typical MIDAS image contains 256 × 240 pixels, the equivalent of some 61 000 individual simultaneous depth profile analyses. Since each pixel corresponds to an area of 1 μm^2, it is possible to determine and correct for local variations in implant depth and concentration by using this system.

The distribution of Ca in plant roots is well-defined (*4*, *14*) and, therefore, this tissue was selected as a model system. The use of an implanted reference element resulted in quantification of the ion microprobe data with an accuracy of 24%. However, it is in the imaging mode that the true potential of ion implantation is realized. By providing an accurate reference element at each point on the ion image, the micrographs can be quantified by applying the calibration line to each point of the MIDAS acquired images. In this manner, the ion micrographs provide not only qualitative distributional information but also quantitative microfeature analysis.

EXPERIMENTAL SECTION

Preparation of Standards. Standards covering a range of calcium concentrations from 1 ppm to 2400 ppm were produced by dissolving measured quantities of calcium 2-ethylhexanoate in Spurr's low viscosity resin (*15*). After curing overnight at 60 °C; 1 μm thin sections were cut from the blocks with an LKB Ultrotome III and mounted on polished silicon wafers for implantation. The calcium concentration of each standard was verified by atomic absorption analysis of the remaining portion of the blocks.

Preparation of Biological Soft Tissue Samples. Two areas of the roots of *Vicia faba* (broad beans) were selected for analysis. One- to two-millimeter samples were collected approximately 1 mm from the root tip and at a distance of 10 mm from the tip. These samples were chemically fixed for 1 h by using 5% gluteraldehyde in 0.03 M Pipes buffer [1,4-piperazinediethanesulfonic acid] at pH 6.8 (*16*). The samples were then washed with 0.15 M Pipes buffer and post fixed for 1 h in 1% OsO_4 in the same buffer. After dehydration in a series of acetone (70–100%) and

0003-2700/83/0355-1959$01.50/0

propylene oxide solutions, the tissue was embedded in Spurr's low viscosity resin and cured overnight at 60 °C. Once again, 1 μm thin sections were cut and mounted on silicon wafers for implantation. The remaining portion of the embedded tissue was analyzed by atomic absorption spectrometry.

Ion Implantation. Ion implantation was performed with an Accelerators Inc. Model 300R ion implanter operating with a hot filament ion source. BF_2^+ ions were generated from BF_3 gas and implanted into the sample and standards by using an energy of 45 kV to a total dosage of 1×10^{15} atoms/cm^2 as determined by target current integration. The implant ion beam current was limited to 2 μA rastered over a 2 in. square area to avoid specimen damage due to target heating.

Ion Microanalysis. All analyses were performed with a CAMECA IMS-3f (*17*) ion microscope/microprobe, operating with a 5.5-kV O_2^+ primary beam and monitoring positive secondary ions. A primary beam current of 750 nA was rastered over an area of 250 × 250 μm. Microprobe analysis of the high Ca concentration standards required the use of lower beam currents to avoid saturation of the electron multiplier used for ion detection. The spectrometer energy slits were set for the maximum energy band-pass of 130 eV and the 150 μm image field transfer optics were used.

Image Acquisition. The microscopic image digital acquisition system (MIDAS) was used to record the images directly from the ion microscope. This system consists of a low light level TV camera, a digital frame buffer (256 × 240 × 12 bit image array) and a graphics display monitor. The framebuffer is interfaced to a Digital Equipment Corp. PDP-11/34A computer which provides more sophisticated image processing capabilities as well as image storage. The image array of the MIDAS system corresponded to a circular area of the sample, 125 μm in diameter. A further description of the system can be found in ref 13 and 18.

Software. Ion probe data were acquired by using manufacturer supplied software for the dedicated HP9845T microcomputer of the CAMECA IMS-3f. The data were subsequently passed to the PDP 11/34A computer for processing with a Fortran IV program which determined the implant range, standard deviation, peak signal intensity, and concentration at the implant peak.

Image data were acquired and processed by using a combination of Fortran IV and assembly language programs on the PDP-11/34A. The image acquisition program uses the frame buffer to sum an operator defined number of images and then outputs the integrated image to disk storage at a rate of up to 1 image every 8 s. Calcium ion images were acquired with a 2-s integration time (60 frame summation) while the less intense boron implant images required a 5-s integration time.

Images were processed by use of the Fortran program IONPIX (*19*). This program performs a variety of functions including image registration and the division and multiplication of images either by a constant or by another image. IONPIX also is capable of performing image registration by cross-correlating the Fourier transform of two images of the same area. Registration can also be done manually by using a routine which superimposes two images, each in a different color, on the video display. The operator can then instruct the program to shift one image relative to the other until the best registration is achieved.

Additional subroutines were written to convert image intensity to ion intensity by using an empirical calibration equation and also to characterize the ion implant profile at each pixel. The latter subroutine, IMPRO, uses the implant image series to determine the maximum signal intensity and the standard deviation of the implant at each pixel. For a Gaussian implant distribution, the standard deviation is defined as the half-width of the implant peak at 0.606 of the peak signal intensity. Therefore, the IMPRO subroutine records the elapsed time between the image which contains the peak intensity for each pixel and the image in which the intensity of that pixel first drops by 39.4% or more.

The final processing program, DISCOR, determines the differential sputtering rates of the sample. This program uses a series of ion images of the substrate, in this case, silicon, to generate a map of the amount of time, $t(x,y)$, required to sputter through the sample to the substrate at each location of the image. A pixel is defined as having completely sputtered away when its image intensity at mass 28 reaches a level of 90% of the intensity

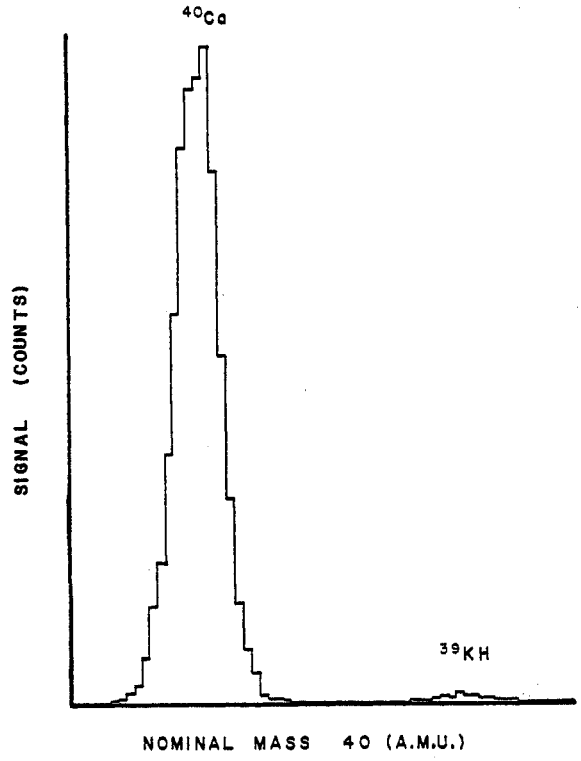

Figure 1. High mass resolution spectra of nominal mass 40 in embedded bean root. Interference of $^{40}Ca^+$ by $^{39}KH^+$ is negligible. Resolution is approximately 4500.

observed at that pixel when imaging a class piece of silicon under identical analysis conditions. This map, and the assumption of a uniform 1 μm section thickness, allows the sputtering rates, $S_r(x,y)$, at each pixel to be computed in cm/s as simply $10^{-4}/t(x,y)$. The assumption of uniform thickness is critical to the use of this correction. A reflecting light microscope was used to screen each section for damage caused by the microtoms or other surface irregularities. In addition, thin sections such as those used in this study often appear colored, as a result of the diffraction of light, with the particular hue being determined by the section thickness. Only sections with uniform coloration were selected for analysis. Due to the necessity for a uniform section, materials which exhibit considerable surface topography, such as freeze-dried sections, are currently unsuitable for use. A further discussion of the DISCOR routine is found in ref 18.

Imaging Procedure. First, a set of boron images which span the depth of the implant zone is acquired. This typically requires approximately 4–5 min; therefore 35 images taken at the maximum transfer rate of 8 s per image are sufficient. Immediately following this, the image of the element of interest, in this case Ca, is acquired. The instrument is then tuned to the substrate mass and the sample is completely sputtered away while another series of images is acquired as input for the DISCOR routine. Since the storage disk will accept a maximum of 80 images, the time between images is increased to between 20 and 30 s. This enables the entire area of analysis to sputter down to the substrate before the storage disk is filled. All images except this last series are then converted from image intensity to ion intensity via an empirical calibration equation.

RESULTS AND DISCUSSION

Before any quantitation of the calcium signal was attempted, the purity of the calcium ion peak was determined by high mass resolution analysis. The high mass resolution spectrum of a section of *Vicia faba* root is shown in Figure 1. It indicates only a weak interference by potassium hydride. All of the standards also showed a negligible interference. Therefore, all further experiments were performed by using low mass resolution to obtain higher sensitivity.

Figure 2 shows the depth profile obtained from an implanted standard. The boron intensity distribution agrees with

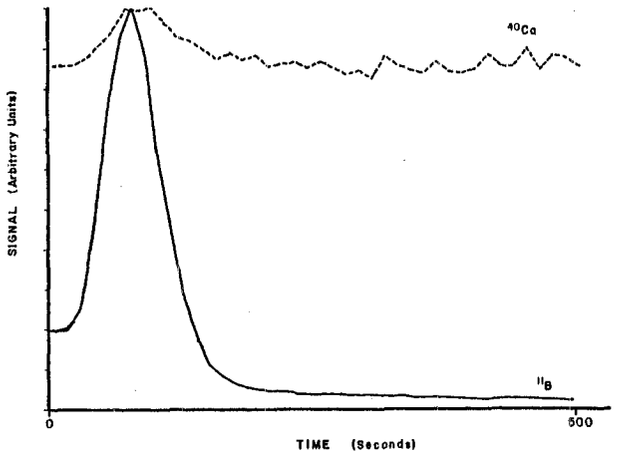

Figure 2. Depth profile of implanted epoxy standard. Sputter rate is 1.2 nm/s.

the expected Gaussian peak shape, and following a slight increase in implant zone the calcium signal remains constant with depth. Boron was chosen as the reference element for two reasons. First, its low mass eliminates mass interference by organic molecular fragments originating from the plastic or tissue. Second, its absence in significant amounts from most biological tissue allows the Gaussian distribution of the implant to be distinguished above any background which may be present.

The BF_2^+ molecular species was used as the implanting ion to obtain the lowest possible energy and thus the shallowest ^{11}B implant obtainable. By implantation of BF_2^+ at 45 kV, an effective ^{11}B implant energy of 10 kV is achieved since the energy of the molecular ion is partitioned among its component atoms according to mass when the ion strikes the target surface. This kept the implant as close to the surface as possible as shown in Figure 2.

The calibration curve was generated from the implanted standards by plotting the ratio of the Ca^+ signal to the peak intensity of the boron implant vs. the concentration of calcium. The curve was linear over a concentration range of 3 to 2000 ppm with a precision of 5–15% at each point. A correlation coefficient of 0.998 was obtained from a least-squares fit. A relative sensitivity factor (RSF) was then computed by using the formula:

$$\mathrm{RSF} = \frac{I_{\mathrm{Ca}}}{I_{\mathrm{B(peak)}}} \frac{[\mathrm{B}]_{\mathrm{peak}}}{[\mathrm{Ca}]} \tag{1}$$

where I_{Ca} and $I_{\mathrm{B(peak)}}$ are the ion intensities of calcium and the boron implant peaks, respectively, [Ca] is the concentration of calcium in parts per million in the plastic standard, and $[\mathrm{B}]_{\mathrm{peak}}$ is the concentration of boron at the implant peak in atoms/cm^3. This latter quantity is easily calculated (*11*) (assuming a Gaussian concentration profile) to be

$$[\mathrm{B}]_{\mathrm{peak}} = F/2.5\sigma \tag{2}$$

where F is the implanted dose in atoms/cm^2 and σ is the standard deviation of the implant peak in centimeters. The boron peak concentration of the standards was found to be 1.06×10^{20} atoms/cm^3, which corresponds to approximately 0.2% by weight.

The accuracy of these standards was then assessed by applying this relative sensitivity factor to quantitatively determine the calcium content of root sections. Results obtained from ion microprobe analysis were compared to the concentrations determined by atomic adsorption spectrometry and are given in Table I. As shown, the ion microprobe agrees within 24% with the atomic absorption analysis. This

Table I. Results of Ion Microprobe Analysis

sample	$^{40}Ca^+$ signal, cps	Ca/B intens ratio	Ca concn, ppm: calcd	Ca concn, ppm: atomic absorption
A1	279 600	2.36	62.1	
A2	533 700	2.42	63.7	
A3	446 900	2.05	53.9	
A4	325 300	2.22	58.4	
$\bar{x}$	396 400 ± 29%	2.26 ± 7%	59.5 ± 7%	49.7
B1	524 700	4.26	112	
B2	834 400	4.64	122	
B3	563 800	4.33	114	
$\bar{x}$	641 000 ± 26%	4.41 ± 5%	116 ± 5%	89.8

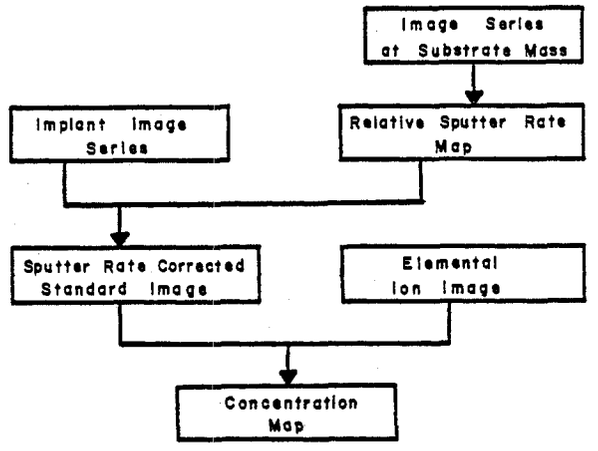

Figure 3. Image quantification schematic.

agreement indicates the absence of any gross matrix effects in the ion microprobe analysis and demonstrates the ability of the implantation technique to provide quantitative data from biological soft tissue.

Although the success of the bulk ion microprobe analysis is unique in itself, the real potential of the ion implantation technique lies in quantitative ion imaging. The procedure employed for converting raw ion image data into concentration maps involves three general steps: (i) characterization of the implant, (ii) determination of relative sputtering rates, and (iii) the final correction to concentration. This procedure is shown schematically in Figure 3 and must be performed for each pixel of the image.

The first two steps in the quantification scheme are to convert the standard deviation given by the subroutine IMPRO to actual sputtered depth and to calculate the implant peak concentration for each pixel. IMPRO calculates the standard deviation as a function of time, $t(x,y)$ (seconds), and this must be converted to actual sputtered depth $\sigma(x,y)$ (centimeters). This conversion is accomplished by using the results of the DISCOR subroutine. As discussed, DISCOR generates a map of the sputter rate for each pixel, $S_r(x,y)$ (cm/s). Thus, a map of the implant standard deviation as actual sputtered depth is obtained by

$$\sigma(x,y)(\mathrm{cm}) = t(x,y)(\mathrm{s})\ S_r(x,y)(\mathrm{cm/s}) \tag{3}$$

Once the standard deviation for each pixel is known, it is possible to calculate the boron peak concentration at each pixel by using eq 2. The end result of the first two steps then is the creation of two maps, one of which is the peak intensity of the implant at each pixel $I_{\mathrm{B(pk)}}(x,y)$ and other the peak concentration at each pixel $[\mathrm{B}]_{\mathrm{pk}}(x,y)$.

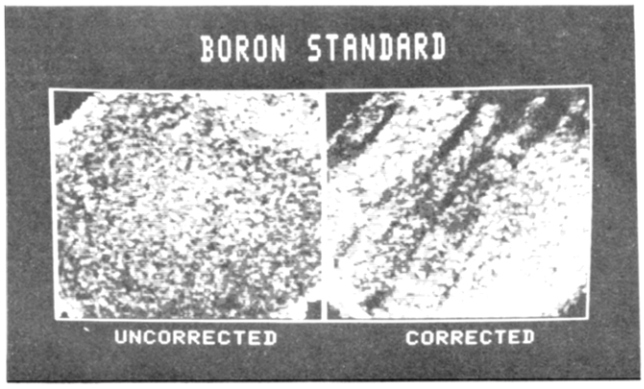

Figure 4. Boron implant peak concentration-to-peak intensity ratio maps: (left) uniform sputter rate assumed for calculation of peak concentration; (right) actual sputter rates used for this calculation. Both images are linearly scaled from 0 to 255. Imaged area is 125 μm in diameter.

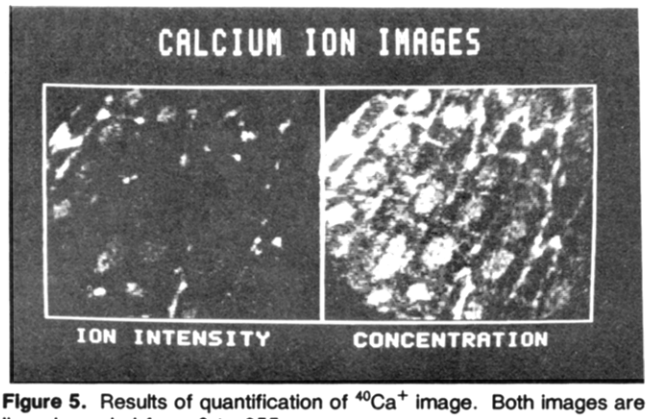

Figure 5. Results of quantification of $^{40}Ca^{+}$ image. Both images are linearly scaled from 0 to 255.

These two maps are then used in the final quantification of the calcium image. Rearranging eq 1 gives

$$[\mathrm{Ca}]_{x,y} = \frac{I_{\mathrm{Ca}(x,y)}}{\mathrm{RSF}} \times \frac{[\mathrm{B}]_{\mathrm{pk}(x,y)}}{I_{\mathrm{B(pk)}(x,y)}} \qquad (4)$$

The latter term is obtained by dividing the two maps generated in the previous steps. Thus, the calcium image is quantified by using a pixel-by-pixel application of the methodology which was applied to the bulk ion microprobe data previously.

The results of the quantification procedure are shown in Figures 4 and 5. Figure 4 shows the results of the implant characterization. The images shown are actually maps of the ratio of implant peak concentration to peak ion intensity at each pixel. The uncorrected image on the left shows the ratio when a uniform sputter rate is assumed. This is equal to a constant divided by the raw boron peak intensity map. The image shows little if any detail and is dominated by the nonhomogeneous microchannel plate response.

In contrast to this the corrected image on the right, produced by using the actual spatially variant sputter rates as determined by DISCOR, shows some cellular detail. In particular, cell walls are distinguishable as lines of somewhat less intensity. These features are shown by DISCOR to be the fastest sputtering regions and therefore, if left uncorrected, will show an erroneously high ion intensity, since ion intensity is assumed to be directly proportional to sputter rate. The corrected image has incorporated the effects of differential sputtering rates; however, the nonuniform response of the microchannel plate is still evident.

Figure 5 gives the final results of the correction procedure. The raw ion intensity image on the left is dominated by several high intensity areas to such an extent that most of the remainder of the image appears dark. The application of the quantification routine is effective in reducing these high intensities and produces a more homogeneous image. The image degradation introduced by the microchannel plate is also substantially reduced by the ratio procedure.

The accuracy of this procedure was assessed by comparing the average concentration of an image obtained by using the image quantification procedure to that given by bulk microprobe analysis of a serial section of root tissue. The bulk ion microprobe analysis yielded a concentration of 120 ppm, while the average image intensity was 70 ppm, a difference of 42%. The real utility of image quantification, however, is its ability to provide concentration data from selected microfeatures. For this case, while the cytoplasm exhibits concentrations of less than 50 ppm, the cell walls and nuclei are found to contain an average of 130 and 150 ppm, respectively.

One important result of this study is the identification of the differential sputtering rate to be a major source of error in quantitative analysis of these plastic embedded tissues. The bulk ion microprobe analyses presented in Table I show the ion microprobe to consistently produce concentrations which are higher than those determined by atomic absorption analysis. The use of quantitative image analysis indicates that this is a systematic error caused by differential sputtering effects.

The ion images reveal as expected (*4*, *14*) that calcium is concentrated predominantly in the nuclei and cell walls, with very little contribution from the cytoplasm. The results of differential sputtering studies in this laboratory (*18*) indicate that these features sputter 15 to 50% faster than the surrounding cytoplasm and epoxy embedding material. The assumption that secondary ion signal intensity is directly proportional to sputter rate would cause the measured secondary ion signal to be higher from these areas than that given by the more slowly sputtering epoxy standards for an equivalent concentration and would thus yield a spuriously high concentration value.

The procedure for image quantification removes the effects of differential sputtering and therefore should not be subject to this error. The data support this conclusion as the application of the differential sputter rate correction to the image results in a lowering of the average concentration of the image by 20% when compared to the results of image quantification by using a spatially invariant sputter rate of 1.2 nm/s (the sputter rate of the epoxy standards). This decrease is close to the amount by which the bulk ion microprobe values were in error. It also agrees with the degree of signal enhancement which would be expected based on the differential sputter rates found in previous experiments.

One drawback of this technique is its requirement for sputtering a large volume of material while acquiring the implant data. The possibility of sputter induced topography or diffusion of the element of interest and their effects on the resultant ion image cannot be ignored. In order to gauge these effects, a series of calcium ion micrographs of root tissue was recorded over the course of 8 min of sputtering. The correlation coefficients of each successive image with the first image of this series were then computed according to the method described in ref 20. For comparison, the correlation coefficients of three successive images of a copper–aluminum focusing grid were also obtained by using the same image acquisition conditions. This provided a standard image which would not be expected to significantly change over the course of the 16 s required to acquire the three images. It therefore serves as a measure of system noise.

The results for the calcium image are plotted in Figure 6, which shows that while degradation in terms of an exact match between the first image and each successive image does occur,

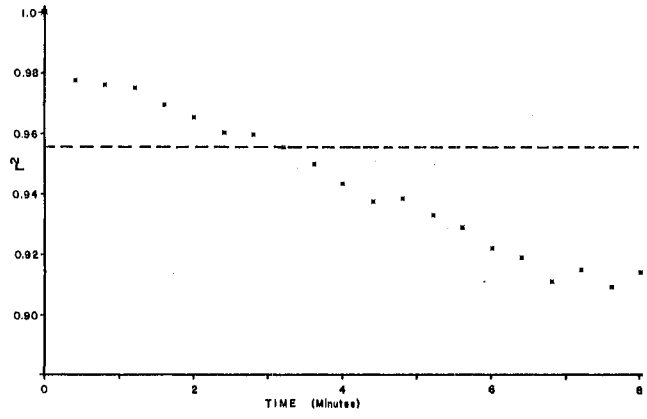

Figure 6. r^2 correlation of successive images vs. time.

it does not become significantly greater than the system noise until 6 min have elapsed. This is longer than the analysis time. Thus, while sputtering does change the ion image, it does not appear to seriously affect these samples.

At present, however, the system noise is a limiting factor. Since the implanted ion dose must be kept low to avoid gross damage to the tissue, and due to the need to detect small concentrations of elements, the imaging system must perform well at high gains. Methods for noise reduction, either through hardware modifications such as high-performance microchannel plates or with the use of appropriate noise filtering software, will provide increased sensitivity.

A second current limitation is the speed at which images can be transferred to disk storage. At the sputtering rate of 1.2 nm/s used in these experiments, a minimum of 9.6 nm of material was eroded between images. The use of a videotape or videodisk unit would allow characterization of the implant with much improved depth resolution by providing real time image storage.

In summary, the merging of quantitative ion implantation, with its ability to provide a laterally homogeneous reference element in an otherwise heterogeneous material, and the MIDAS image acquisition system's unique capability for characterizing this implanted reference element at each discrete location of the ion image provides a powerful tool for quantitative ion microscopy. This study has demonstrated the ability of this combination to provide concentration data on biological soft tissue. The technique is equally applicable to a wide range of heterogeneous materials.

ACKNOWLEDGMENT

The authors are grateful to Sarah Asher for her invaluable assistance throughout the work and to Adam Patkin for his help with the software. The implantation facilities of the National Research and Resource Facility for Submicron Structures at Cornell were used.

Registry No. Ca, 7440-70-2; B, 7440-42-8; BF_2^+, 12355-90-7.

LITERATURE CITED

(1) Morrison, G. H.; Slodzian, G. *Anal. Chem.* **1975**, *47*, 932A-943A.
(2) Castaing, R.; Slodzian, G. *J. Microsc.* **1962**, *1*, 395-410.
(3) Galle, P.; Blaise, G.; Slodzian G. "IVth National Conference on Electron Microprobe Analysis"; California Institute of Technology: Pasadena, CA, 1969; Vol. 1, p 36.
(4) Galle, P. In "Secondary Ion Mass Spectrometry SIMS-II", Benninghoven, A., et al., Eds.; Springer: New York, 1979; Springer Ser. in Chem. Phys., Vol. 9, p 238.
(5) Spurr, A. K. *Scanning Electron Microsc.* **1980**, *3*, 97-109.
(6) Truchet, M.; Trottier, S. *C. R. Acad. Sci., Ser. D* **1979**, *288*, 831-833.
(7) Lodding, A.; Gourgont, J. M.; Peterson, L. G.; Frostell, G. *Z. Naturforsch. A* **1974**, *29*, 897-900.
(8) Burns-Bellhorn, M. S.; File, D. M. *Anal. Biochem.* **1979**, *92*, 213-221.
(9) Zhu, D.; Harris, W. C.; Morrison, G. H. *Anal. Chem.* **1982**, *54*, 419-422.
(10) Gries, W. H.; Rautenbach, W. L. 6th International Symposium on Microtechniques, Graz, Austria 1970.
(11) Leta, D. P.; Morrison, G. H. *Anal. Chem.* **1980**, *52*, 277-280.
(12) Leta, D. P.; Morrison, G. H. *Anal. Chem.* **1980**, *52*, 514-519.
(13) Furman, B. K.; Morrison, G. H. *Anal. Chem.* **1980**, *52*, 2305-2310.
(14) Chandra, S.; Chabot, J. F.; Morrison, G. H.; Leopold, A. C. *Science* **1982**, *216*, 1221-1223.
(15) Spurr, A. R. *J. Ultrastruct. Res.* **1969**, *26*, 31-43.
(16) Salema, R.; Brando, I. *J. Submicrosc. Cytol.* **1973**, *5*, 79-96.
(17) Ruberol, J. M.; Lepareur, M.; Autier, B.; Gourgout, J. M. 8th International Congress on X-Ray Optics and Microanalysis and the 12th Annual Conference of the Microbeam Analysis Society, Boston, MA, 1977.
(18) Patkin, A. J.; Chandra, S.; Morrison, G. H. *Anal. Chem.* **1982**, *54*, 2507-2510.
(19) Fassett, J. D.; Roth, J. R.; Morrison, G. H. *Anal. Chem.* **1977**, *49*, 2322-2329.
(20) Frank, J.; Al-Ali, L. *Nature (London)* **1975**, *256*, 376-379.

RECEIVED for review April 8, 1983. Accepted July 22, 1983. Funding for this project was provided by National Institutes of Health, the National Science Foundation, and the Office of Naval Research.

Relative Sensitivity Factors of Elements in Quantitative Secondary Ion Mass Spectrometric Analysis of Biological Reference Materials

G. O. Ramseyer and G. H. Morrison*

Department of Chemistry, Cornell University, Ithaca, New York 14853

Secondary ion mass spectrometry is applied to the quantitative analysis of homogenized biological reference materials. The technique involves determining relative sensitivity factors ratioed to K for Na, Ca, Mg, B, Mn, Fe, N, P, Al, and Cl, and ratioed to P for Cl, F, CN, and SO in several types of biological matrices.

Secondary ion mass spectrometry (SIMS) is a sensitive technique capable of determining most elements in a broad range of solid samples. Because the sensitivity of an element is a function of the type of matrix in which it is located (*1*), quantitative SIMS determinations are accomplished by either semitheoretical methods or empirical calibration methods using standards (*2-4*). When standards are available which closely approximate that of the sample, relative sensitivity factors (RSF's) have been demonstrated to consistently provide the most accurate results in inorganic matrices (*2-5*).

RSF's have been applied to the elemental determinations in groups of similar inorganic matrices, including glasses (*2, 5, 6*), metals (*6, 7*) and geologicals (*8*). Because of the wide diversity of biological materials and the lack of microstandards, the quantification of biological materials has been more

0003-2700/83/0355-1963$01.50/0